

Supporting Information for:

Architecting carbon coated $\text{Mo}_2\text{CT}_x/\text{MoSe}_2$ heterostructures enable robust potassium storage

Qingqing Jiang,^{*a, #} Weifang Zhao,^{a, #} Xinyue Xu,^a Da Ke,^b Ran Ren,^a Fuzhen Zhao,^a Shilin Zhang,^c Tengfei Zhou,^{*b} Juncheng Hu^{*a}

^a Key Laboratory of Catalysis and Energy Materials Chemistry of Ministry of Education, Hubei Engineering Technology Research Centre of Energy Polymer Materials, School of Chemistry and Materials Science, South-Central Minzu University, Wuhan 430074, China

^b Institutes of Physical Science and Information Technology, Anhui University, Hefei 230601, China

^c School of Chemical Engineering & Advanced Materials, University of Adelaide, Adelaide, SA 5005, Australia

1. Experimental Methods

1.1. Preparation of Mo_2CT_x MXene flakes: Mo_2CT_x flakes were prepared by Ga etching from $\text{Mo}_2\text{Ga}_2\text{C}$ powder in aqueous HF. Specifically, 500 mg $\text{Mo}_2\text{Ga}_2\text{C}$ powder was slowly added into 40 mL HF (49 wt.%) and kept stirring at 58 °C for 7 days. Afterwards, the precipitate was collected by centrifugation and washed several times with deionized water (until pH \approx 6). Finally, the product was dried in a vacuum freeze dryer for 48 h to obtain Mo_2CT_x powder.

1.2. Preparation of $\text{MoSe}_2/\text{Mo}_2\text{CT}_x$ heterostructures: Firstly, Mo_2CT_x powder was dispersed in deionized water and ultrasonic treatment for 3 h under flowing N_2 atmosphere to obtain Mo_2CT_x suspension (1 mg/mL). Subsequently, 40 mg of Se powder was dissolved in 5 mL of $\text{N}_2\text{H}_4 \cdot \text{H}_2\text{O}$ (85 wt.%) by continuously stirring for 1 h. Meanwhile, 61 mg of $\text{Na}_2\text{MoO}_4 \cdot 2\text{H}_2\text{O}$ was dissolved in 20 mL of deionized water to obtain a clarified solution. Then, 15 mL of Mo_2CT_x suspension (1 mg/mL) was added into the Na_2MoO_4 solution under stirring and ultrasonic treatment for 1 h. Afterward, the Se- N_2H_4 solution was added dropwise to the above mixture. The resulting suspension was transferred into a Teflon-lined stainless-steel autoclave and heated at 200 °C for 12 hours. After cooling to room temperature, the product was collected by centrifugation and washed with deionized water for several times. Finally, $\text{MoSe}_2/\text{Mo}_2\text{CT}_x$ powder was obtained by drying overnight at 60 °C in a vacuum oven. In addition, other samples with different mass ratio

(MoSe₂ to Mo₂CT_x) were prepared, including 1/2-MoSe₂/Mo₂CT_x-5 (20 mg Se powder, 30 mg Na₂MoO₄·2H₂O and 5 ml Mo₂CT_x suspension), 2-MoSe₂/Mo₂CT_x-5 (79 mg Se powder, 121 mg Na₂MoO₄·2H₂O and 5 ml Mo₂CT_x suspension), MoSe₂/Mo₂CT_x-5 (5 ml Mo₂CT_x suspension) and MoSe₂/Mo₂CT_x-10 (10 ml Mo₂CT_x suspension).

1.3. Preparation of MoSe₂/Mo₂CT_x@C: 45 mg of MoSe₂/Mo₂CT_x powder was dispersed in 80 mL of Tris-buffer solution (10 mM) by ultrasonic treatment for 1 h. Next, 25 mg of dopamine hydrochloride was quickly added to the mixed solution. After continuous stirring for 3 h, the black precipitate was collected by centrifugation and washed with deionized water. Subsequently, MoSe₂/Mo₂CT_x@PDA was obtained by vacuum drying overnight at 60 °C. Finally, the MoSe₂/Mo₂CT_x@PDA were placed in a tube furnace and heated at 600 °C for 2 h to obtain MoSe₂/Mo₂CT_x@C.

1.4. Preparation of Mo₂CT_x/Se: The Se powder and Mo₂CT_x powder were placed at the upstream and downstream of the tube furnace in two separate ceramic boats, respectively. The weight ratio of sample to selenium powder was 1:1.5. Then, the temperature was elevated to 600 °C with a heating rate of 5 °C min⁻¹ and the reaction was kept at 600 °C for 2 h to obtain Mo₂CT_x/Se samples.

1.5 Materials Characterization

Scanning electron microscopy (SEM) was performed with a field-emission scanning electron microscope (Hitachi SU-8010, Japan) operated at a deceleration voltage of 1.5 kV to characterize the morphologies of the products. Transmission electron microscopy (TEM) images were taken with a JEOL JEM-2010 LaB6 high-resolution transmission electron microscope operated at 200 kV. High-resolution (HRTEM) images were taken with a JEOL JEM-2100F field-emission high-resolution transmission electron microscope operated at 200 kV. X-ray diffraction (XRD) patterns were recorded with a D8 Advance X-ray diffractometer (Bruker AXS company, Germany) equipped with a Cu-K α radiation source ($\lambda=1.5406$ Å). A DXR Raman confocal microscope (Thermo Fisher Scientific, USA) with a 532 nm @10 mW Laser was used to record Raman spectra. X-ray photoelectron spectroscopy (XPS) measurements (VG Multilab 2000 photoelectron spectrometer) was performed with a Al K α radiation as the excitation source under a 2×10^{-6} Pa vacuum; the C 1s peak of the surface adventitious carbon at 284.6 eV was used to calibrate all of the binding energies.

1.6 Preparation of Electrolyte

The electrolyte system including 3M KFSI (DME) and 3M KFSI (EC/DEC) were prepared by dissolving a certain amount of potassium salt (KFSI) into different solvents, including carbonate-based solvents (EC+DEC, 1 : 1 volume ratio), and ether-based solvents (DME) in an argon-filled glove box (O₂ < 0.1 ppm, H₂O < 0.1 ppm).

1.7 Electrochemical Characterization

The electrochemical tests were carried out using CR2032 coin-type cells. The working electrodes were prepared by mixing the active materials, Ketjen black, and polyvinylidene fluoride (PVDF), at a weight ratio of 70 : 20 : 10, which was then pasted on a copper foil. For half PIBs, K metal was used as the counter and reference electrode, and a polypropylene membrane (Celgard 2400) was used as the separator. Cell assembly was performed in an argon-filled glovebox. The mass loading of active material in the working electrode was about 0.8-1.0 mg cm⁻², and the diameter of the working electrode was 8 mm. The amount of electrolyte for each coin battery is around 240 μL. The charge and discharge tests were conducted with a NEWARE battery tester. Cyclic voltammograms (CVs) in a voltage range of 0.01-3 V and electrochemical impedance spectroscopy (EIS) spectrum were performed with an electrochemical workstation (IviumStath., Ivium Holland, Inc.). Electrochemical impedance spectra were obtained in the frequency range of 100 kHz-0.01 Hz with an amplitude of 5 mV. Galvanostatic intermittent titration technique (GITT) tests were recorded with a NEWARE battery tester in the potential range of 0.01-3 V at ambient temperature. After charge-discharge for 20 cycles, GITT measurements were carried out at a low current density of 50 mA g⁻¹ for 0.5 h followed by a rest interval of 2 h.

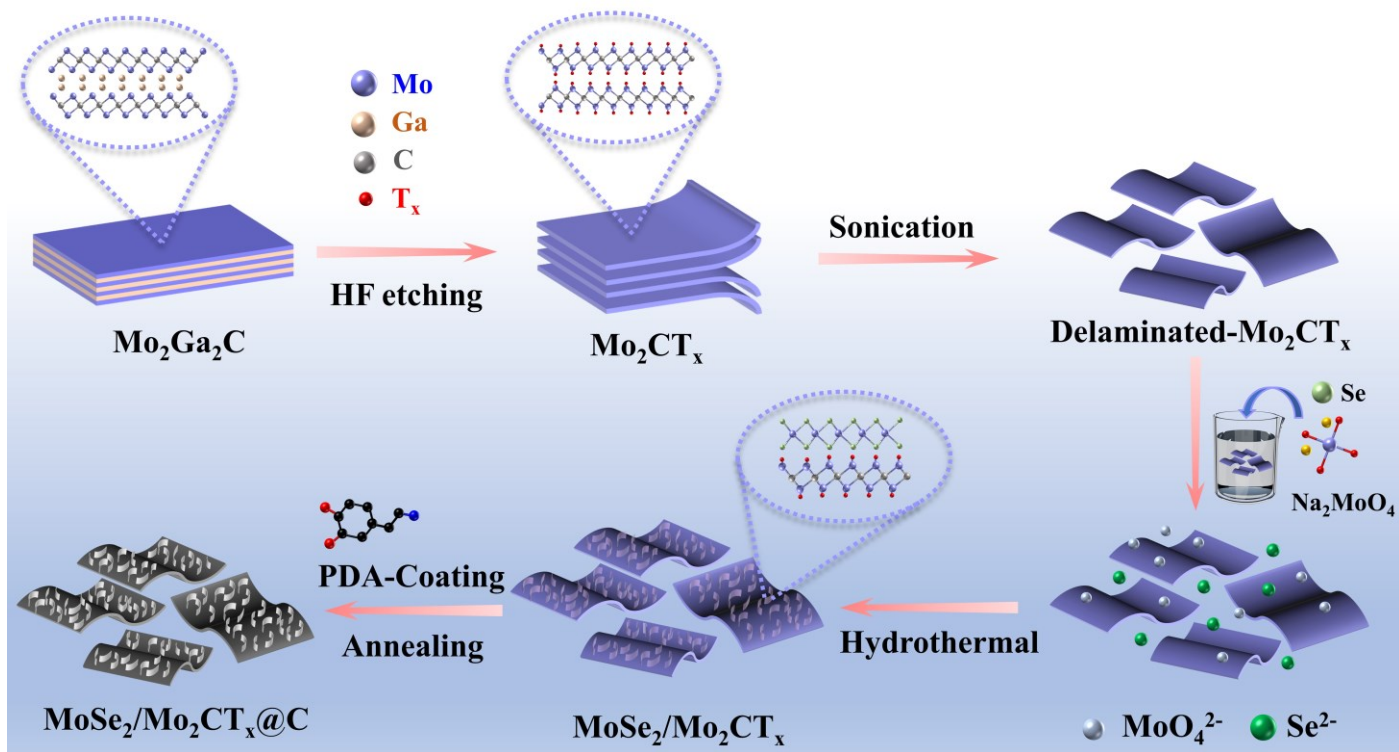


Fig. S1 Detailed schematic of the synthesis procedures of $\text{MoSe}_2/\text{Mo}_2\text{CT}_x@C$.

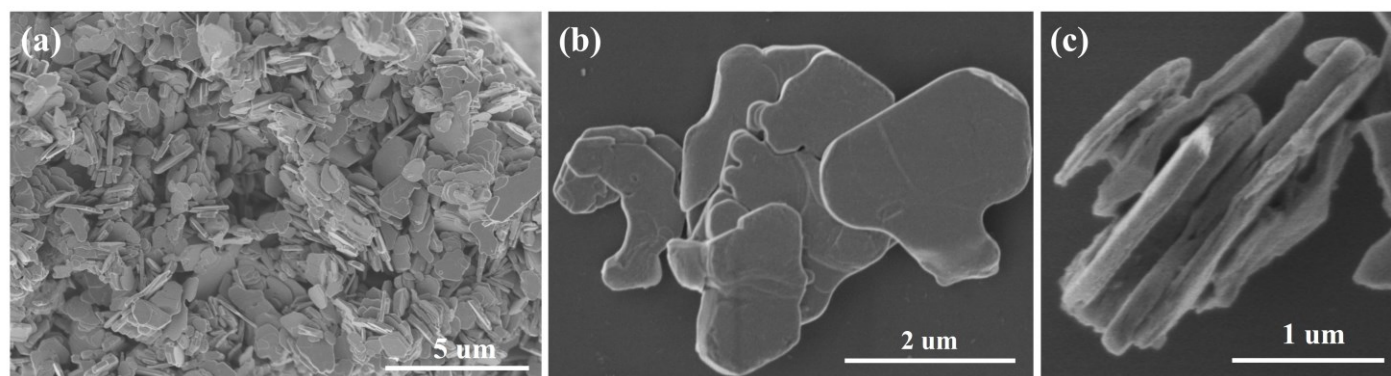


Fig. S2 SEM images of Mo_2CT_x MXenes.

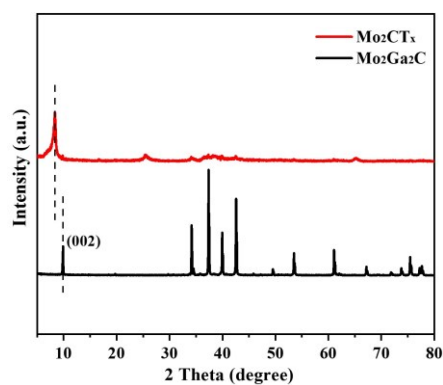


Fig. S3 XRD patterns of $\text{Mo}_2\text{Ga}_2\text{C}$ MAX and Mo_2CT_x MXenes.

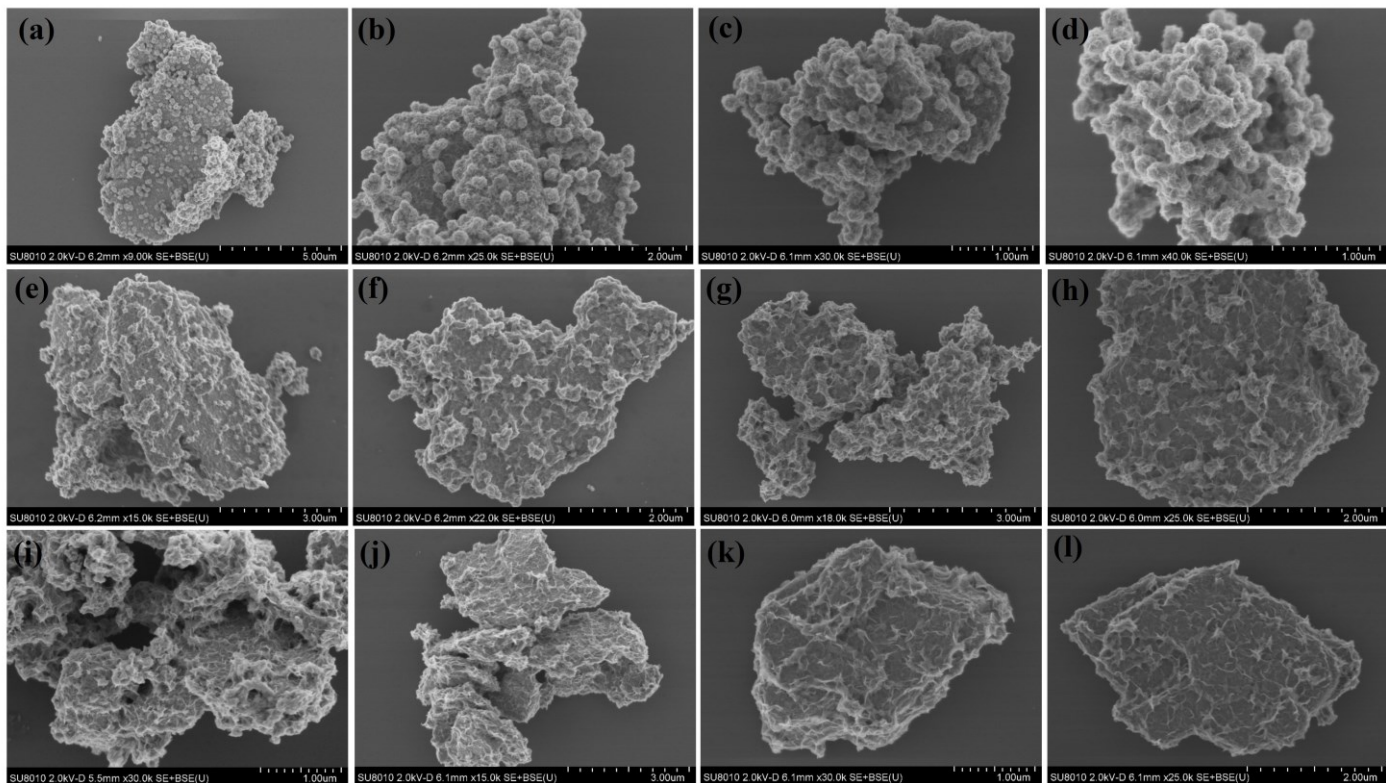


Fig. S4 SEM images of (a-d) $\text{MoSe}_2/\text{Mo}_2\text{CT}_x-5$, (e-h) $\text{MoSe}_2/\text{Mo}_2\text{CT}_x-10$, (i-l) $\text{MoSe}_2/\text{Mo}_2\text{CT}_x-15$.

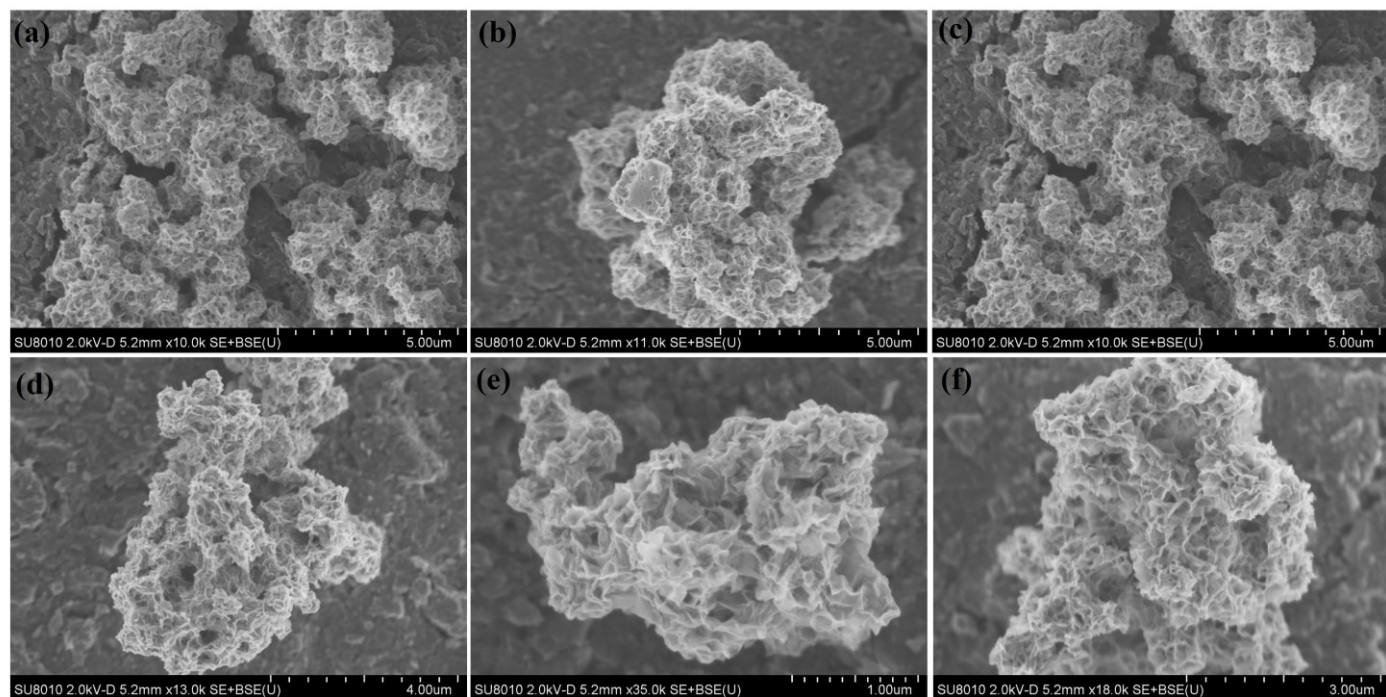


Fig. S5 SEM images of (a-c) $1/2\text{-MoSe}_2/\text{Mo}_2\text{CT}_x-5$, (d-f) $2\text{-MoSe}_2/\text{Mo}_2\text{CT}_x-5$.

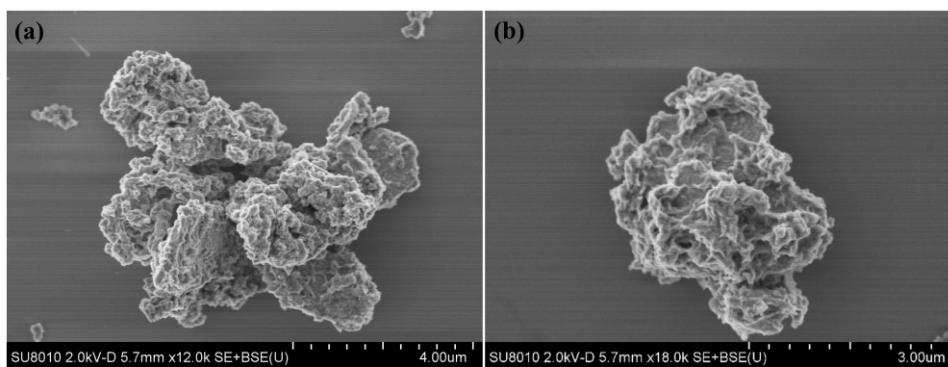


Fig. S6 SEM images of $\text{MoSe}_2/\text{Mo}_2\text{CT}_x@\text{C}$.

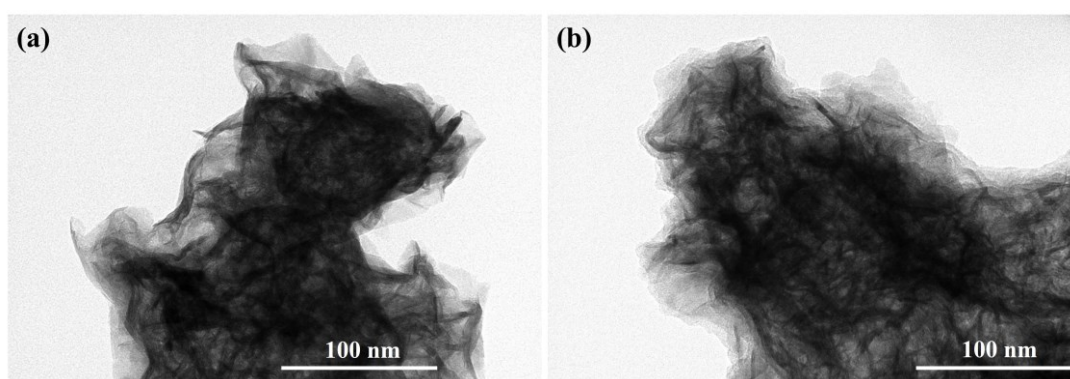


Fig. S7 TEM images of (a) $\text{MoSe}_2/\text{Mo}_2\text{CT}_x$, (b) $\text{MoSe}_2/\text{Mo}_2\text{CT}_x@\text{C}$.

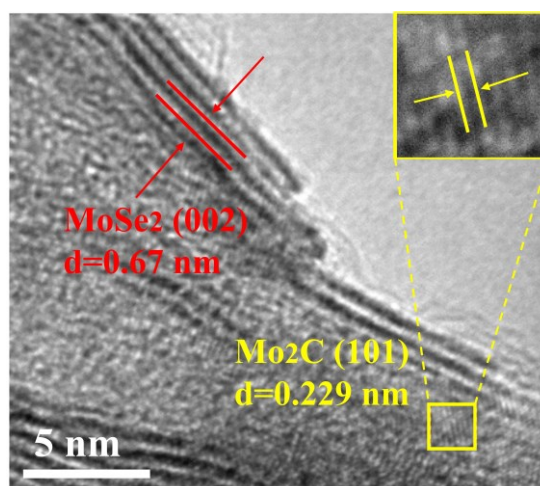


Fig. S8 HRTEM images of $\text{MoSe}_2/\text{Mo}_2\text{CT}_x@\text{C}$.

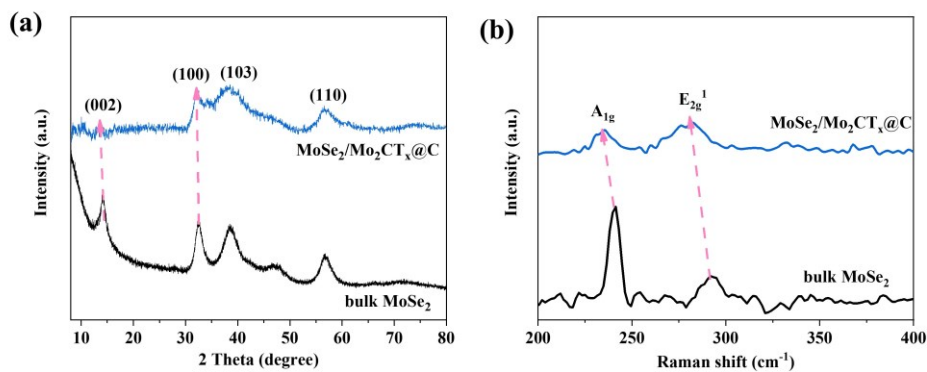


Fig. S9 (a) XRD pattern and (b) Raman spectrum of bulk MoSe₂ and MoSe₂/Mo₂CT_x@C.

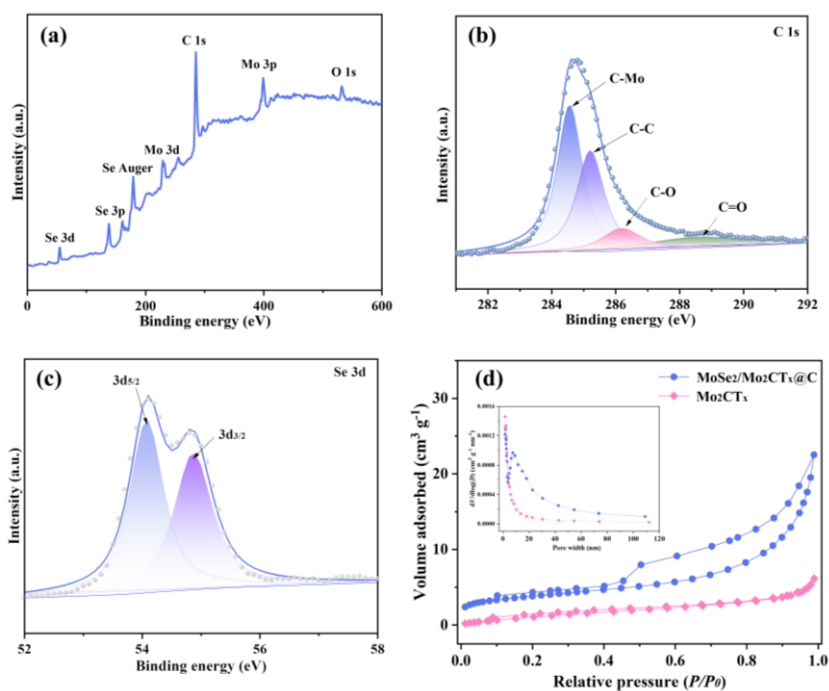


Fig. S10 (a) XPS survey of MoSe₂/Mo₂CT_x@C. XPS spectrum of (b) C 1s, (c) Se 3d in MoSe₂/Mo₂CT_x@C. (d) N₂ adsorption and desorption isotherm and pore-size distribution of pure Mo₂CT_x and MoSe₂/Mo₂CT_x@C.

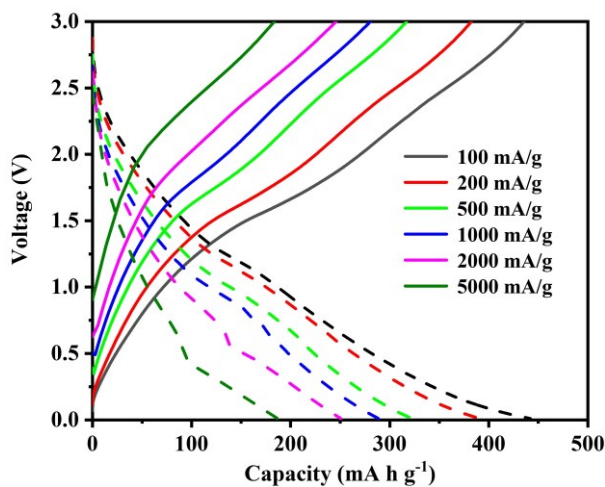


Fig. S11 GDV curves of MoSe₂/Mo₂CT_x@C electrode at different current density.

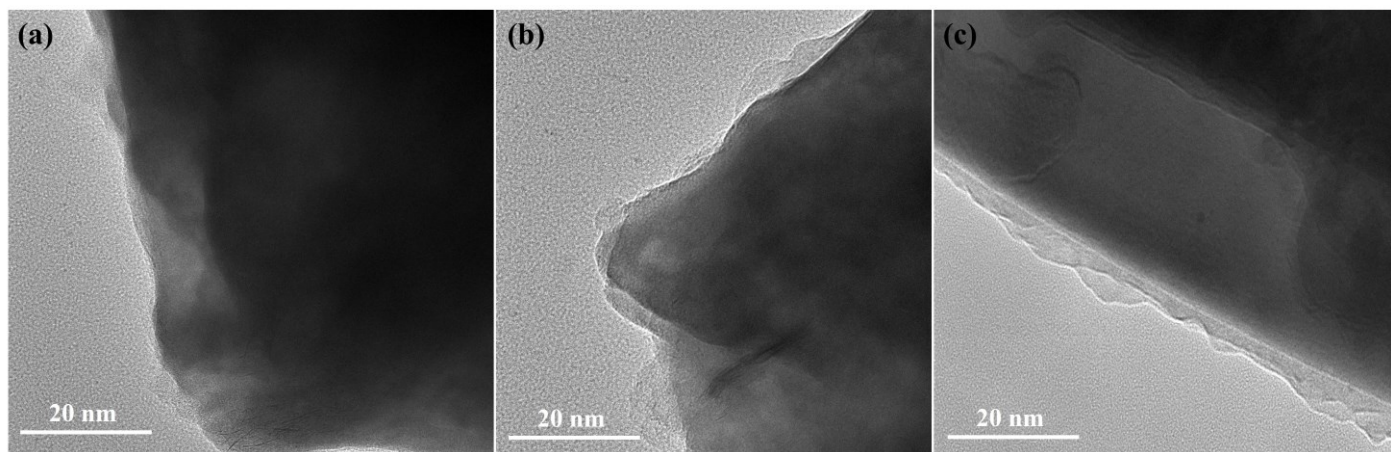


Fig. S12 SEI films for (a) $\text{MoSe}_2/\text{Mo}_2\text{CT}_x$ electrode and (b-c) $\text{MoSe}_2/\text{Mo}_2\text{CT}_x@\text{C}$ electrode.

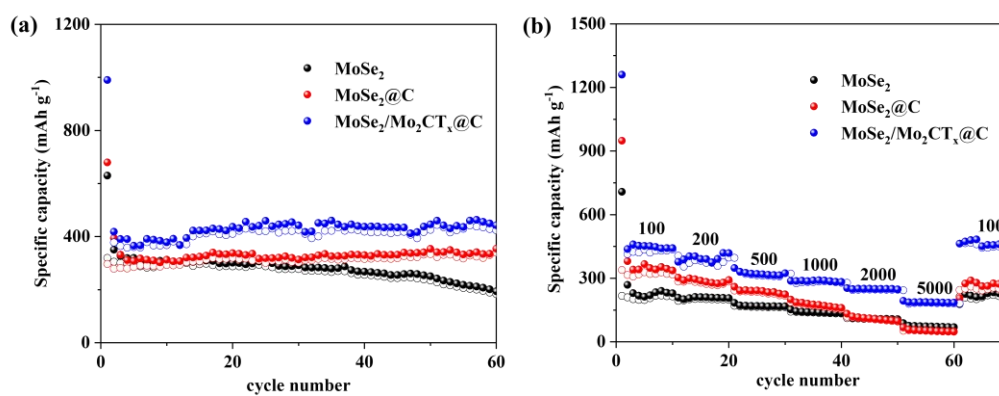


Fig. S13 The (a) cycling performance at 100 mA g^{-1} and (b) rate performance at 100 mA g^{-1} , 200 mA g^{-1} , 500 mA g^{-1} , 1000 mA g^{-1} , 2000 mA g^{-1} and 5000 mA g^{-1} of MoSe_2 , $\text{MoSe}_2@\text{C}$ and $\text{MoSe}_2/\text{Mo}_2\text{CT}_x@\text{C}$.

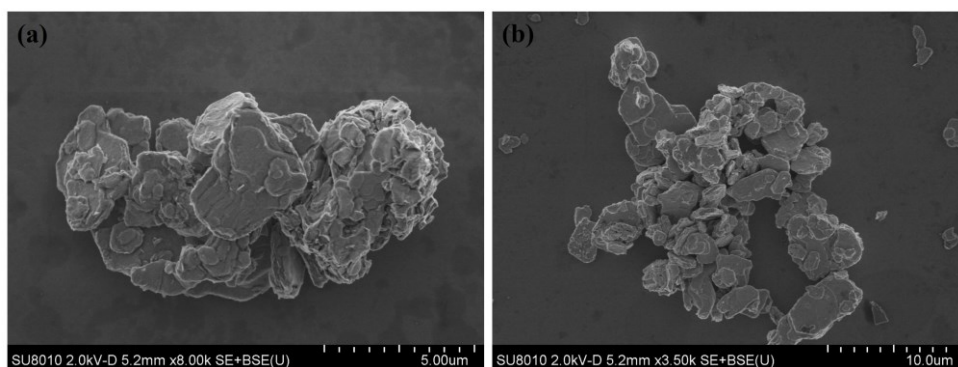


Fig. S14 SEM images of $\text{Mo}_2\text{CT}_x/\text{Se}$ nanohybrids.

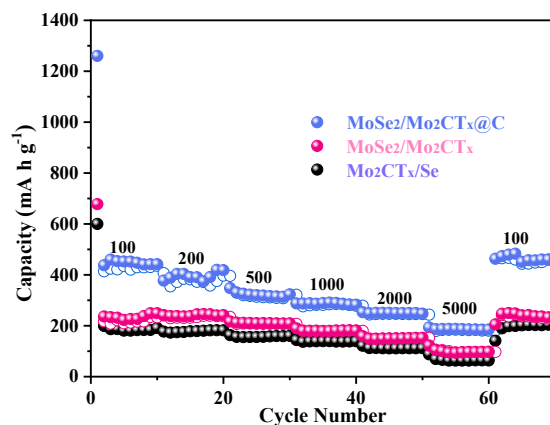


Fig. S15 Comparison of rate performance for $\text{Mo}_2\text{CT}_x/\text{Se}$, $\text{MoSe}_2/\text{Mo}_2\text{CT}_x$ and $\text{MoSe}_2/\text{Mo}_2\text{CT}_x@\text{C}$.

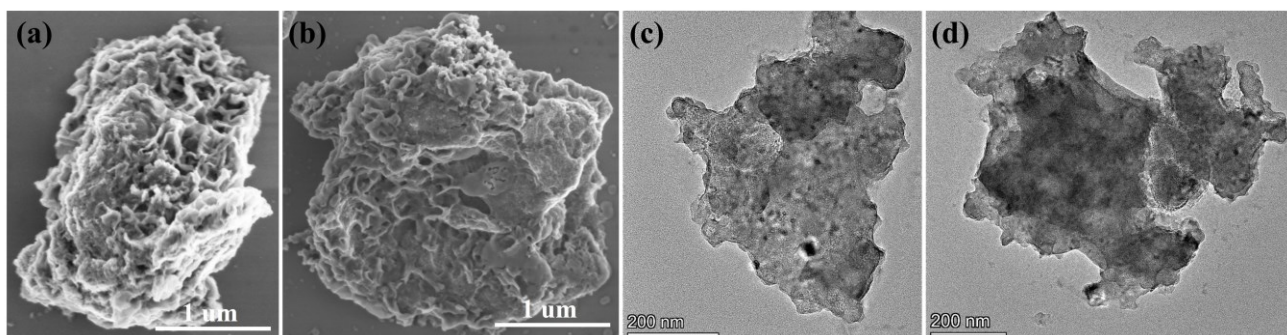


Fig. S16 Ex-situ (a-b) SEM and (c-d) TEM of $\text{MoSe}_2/\text{Mo}_2\text{CT}_x@\text{C}$ electrode after 500 cycles at 2000 mA g^{-1} .

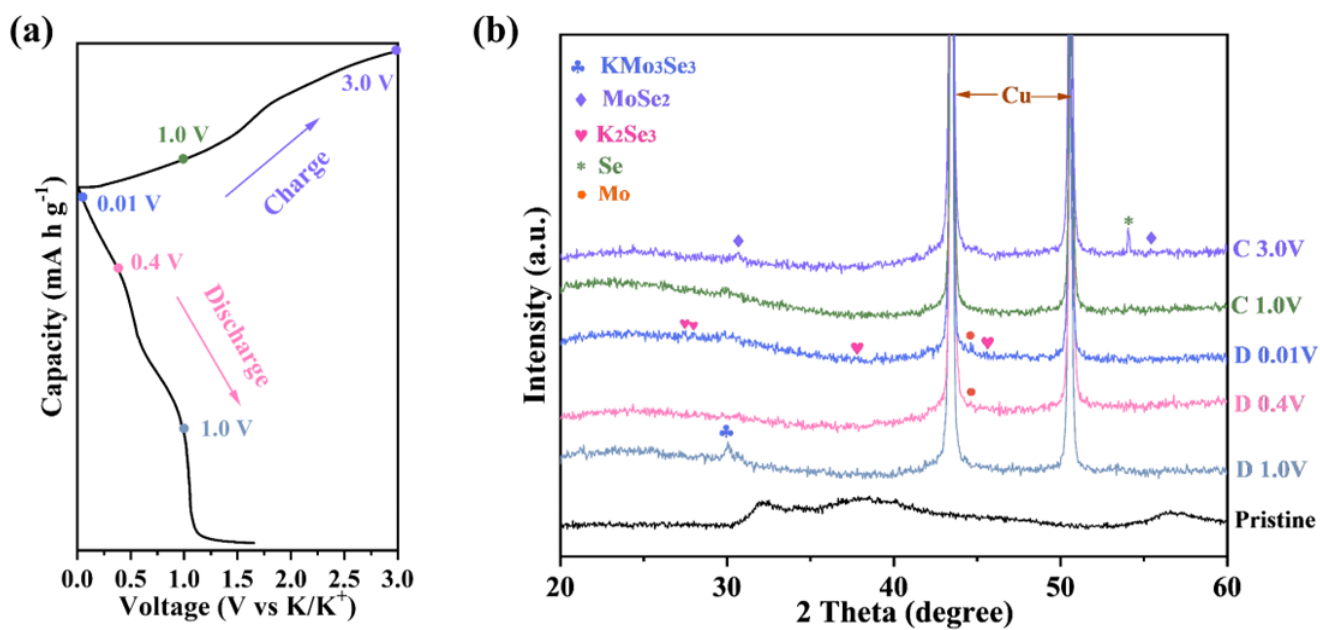


Fig. S17 (a) Illustration of the charge and discharge states. (b) Ex situ XRD patterns at various charge and discharge states.

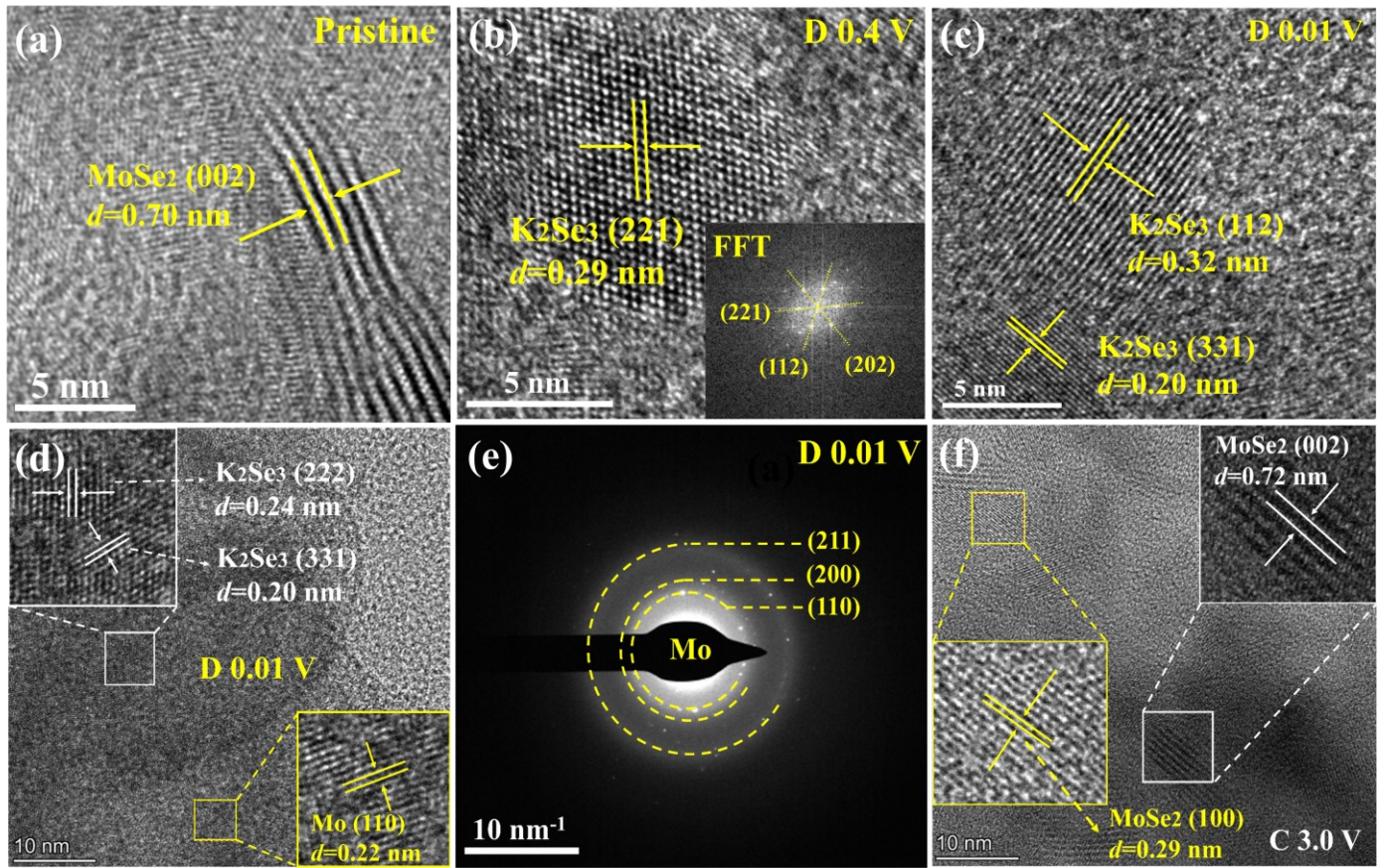
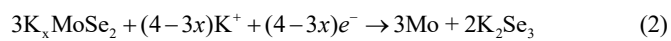
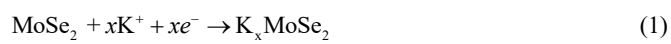


Fig. S18 (a-f) Ex-situ HRTEM images of MoSe₂/Mo₂CT_x@C electrode at various charge and discharge stages.

The conversion reaction mechanism of MoSe₂/Mo₂CT_x@C in PIBs could be derived as following based on the above-mentioned analysis:

Discharging:



Charging:

